Electronic Supplementary Material (ESI) for Dalton Transactions.
This journal is © The Royal Society of Chemistry 2021

Cyclometalated Ir(III) complexes as potential electron acceptors for organic solar cells

Tianjian Yang,†[a] Yinming He,†[a] Yang Cheng,†[a] Xuyu Gao,[a] Yijing Wu,[a] Wenbo Yuan,[a] Youtian Tao*[a]

[a] *Key lab for Flexible Electronics and Institute of Advance Materials, Jiangsu National Synergistic Innovation Center for Advanced Materials (SICAM), Nanjing Tech University, 30 South Puzhu Road, Nanjing 211816, People's Republic of China.*

E-mail: iamyttao@njtech.edu.cn

†These authors contributed equally to this work.

General measurements and characterization

^{1}H NMR spectra were measured using a Bruker DMX-500 spectrometer in deuterochloroform with tetramethylsilane (TMS; δ=0 ppm) as an internal standard. Mass spectra were measured using a Bruker Autoflex matrix assisted laser desorption/ionization time-of-flight (MALDI-TOF). Elemental analysis (EA) of C, H, N and S were measured by a Vario EL Ⅲ micro analyzer. Ultraviolet-visible (UV-vis) absorption spectra of dilute solution (1 × 10^{-5} M) in chloroform and thin film on a quartz substrate were measured using Shimadzu UV-2500 recording spectrophotometer. The photoluminescence (PL) spectra and transient lifetime was recorded using Edinburgh FLS-980 instrument in thin film state. Thermal gravimetric analysis (TGA) was measured with a METTLER TOLEDO TGA2 instrument. The electrochemical cyclic voltammetry was conducted on a CHI voltammetric analyzer, in a 0.1 mol L^{-1} acetonitrile solution of tetrabutylammonium hexafluorophosphate (n-Bu_4NPF_6) at a potential scan rate of 100 mV s^{-1}. The conventional three electrode configuration consists of a platinum working electrode, a platinum wire counter electrode, and an Ag/AgCl wire pseudo-reference electrode. The polymer sample was coated on the platinum sheet of working electrode. The reference electrode was checked versus ferrocenium-ferrocene (Fc^+/Fc) as internal standard as recommended by IUPAC (the vacuum energy level: -4.8 eV). All the solution were deaerated by bubbling nitrogen gas for a few minutes prior to the electrochemical measurements. HOMO energy levels were calculated from the equation of E_{HOMO} = -(E_{onset}(ox) + 4.8) eV, and LUMO energy were deduced from the optical band gap (E_g) values and HOMO levels. *J-V* curves of OSCs devices were measured using a computer controlled Keithley 2400 Source Measure Unit under a simulated AM 1.5G spectrum, which was obtained by Oriel Sol3A Class Solar Simulator (model, Enlitech SS-F5-3A) with a 450 W xenon lamp and an air mass 1.5 filter. EQE spectra was measured by Solar Cell Spectral Response Measurement System QE-R3-011 (Enli Technology, Taiwan). AFM measurement was performed via Bruker Dimension ICON atomic force microscopy.

Materials and synthetic procedures

Materials: All solvents were obtained commercially and used without further purification. CB and $CHCl_3$ was purchased from Sigma Aldrich Co. PBDB-T was purchased from One-Materials Inc.. 2-(3-ethyl-4-oxothiazolidin-2-ylidene)malononitrile were purchased from Suna Tech. The Ir complexes were synthesized according to the literature report. The detailed synthetic procedures of TR, 2TR, TRIr, and 2TRIr were outlined below.

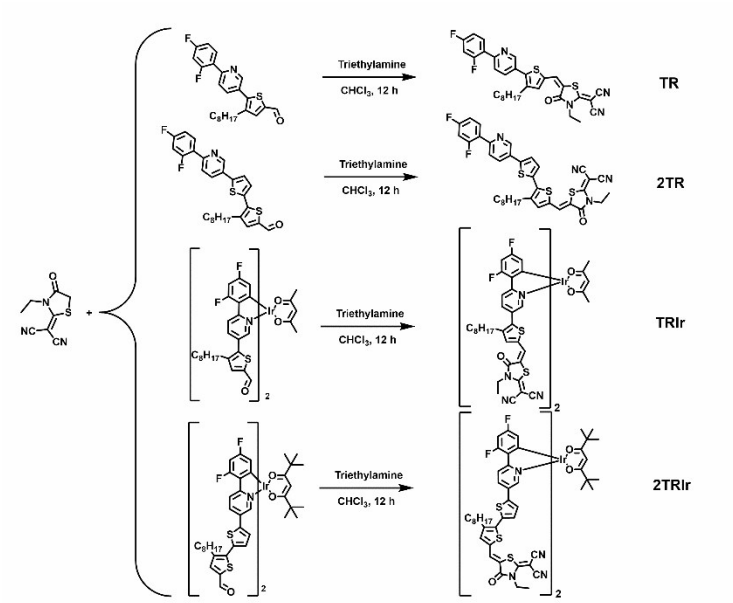

Scheme S1 Synthetic routes of the cyclometalated Ir complexes (TRIr and 2TRIr) and the corresponding organic ligand (TR and 2TR).

Synthesis of TR: 5-(6-(2,4-difluorophenyl)pyridine-3-yl)-4-octylthiophene-2-carbaldehyde dfppyTA (500 mg, 1.21 mmol) and 2-(3-ethyl-4-oxothiazolidin-2-ylidene)malononitrile (280 mg, 1.45 mmol) were stirred in the solvent with a mixture of anhydrous chloroform (30 mL) and triethylamine (0.3 mL) at room temperature for 12 h under a nitrogen atmosphere. Then the precipitate was extracted with CH_2Cl_2:PE (2:1), washed with brine, dried over anhydrous $MgSO_4$, and concentrated under reduced pressure. The crude product was purified by chromatography on silica gel (eluent: dichloromethane) and wash with MeOH to yield the title compound as yellow solid TR (437 mg, 61.4%). ^{1}H NMR (400 MHz, $CDCl_3$), δ (TMS, ppm): 8.81 (dd, *J* = 2.2, 0.9 Hz, 1H), 8.10 (td, *J* = 8.9, 6.7 Hz, 1H), 8.03 (s, 1H), 7.91 – 7.82 (m, 2H), 7.38 (s, 1H), 7.06 – 6.99 (m, 1H), 6.97 – 6.89 (m, 1H), 4.31 (q, *J* = 7.2 Hz, 2H), 2.78 – 2.63 (m, 2H), 1.63 (dt, *J* = 15.5, 7.7 Hz, 2H), 1.40 (t, *J* = 7.2 Hz, 3H), 1.30 – 1.14 (m, 10H), 0.84 (t, *J* = 6.9 Hz, 3H). MALDI-TOF (m/z): M^+ calculated at 588.18, found at 589.31; Anal. Calcd for $C_{32}H_{30}F_2N_4OS_2$: C 65.28, H 5.14, N 9.52, S 10.89%; found: C 65.67, H 4.92, N 9.62, S 10.83%.

Synthesis of 2TR: 5'-(6-(2,4-difluorophenyl)pyridine-3-yl)-3-octyl-[2,2'-bithiophene]-5-carbaldehyde dfppy2TA (500 mg, 1.01 mmol) and 2-(3-ethyl-4-oxothiazolidin-2-ylidene)malononitrile (243 mg, 1.21 mmol) were stirred in the solvent with a mixture of anhydrous chloroform (30 mL) and triethylamine (0.3 mL) at room temperature for 12 h under a nitrogen atmosphere. Then the precipitate was extracted with CH_2Cl_2:PE (2:1), washed with brine, dried over anhydrous $MgSO_4$, and concentrated under reduced pressure. The crude product was purified by chromatography on silica gel (eluent: dichloromethane) and wash with MeOH to yield the title compound as reddish-brown solid 2TR (437 mg, 64.6%). ^{1}H NMR (400 MHz, $CDCl_3$), δ (TMS, ppm): 8.97 (dd, *J* = 2.4, 0.7 Hz, 1H),

8.11 – 8.03 (m, 1H), 7.99 (s, 1H), 7.95 (dd, *J* = 8.3, 2.4 Hz, 1H), 7.83 – 7.79 (m, 1H), 7.42 (d, *J* = 3.9 Hz, 1H), 7.34 (d, *J* = 3.9 Hz, 1H), 7.30 (s, 1H), 7.04 – 6.98 (m, 1H), 6.95 – 6.88 (m, 1H), 4.30 (q, *J* = 7.2 Hz, 2H), 2.87 – 2.81 (m, 2H), 1.74 – 1.63 (m, 2H), 1.41 – 1.38 (m, 3H), 1.33 – 1.21 (m, 10H), 0.89 – 0.82 (m, 3H). MALDI-TOF (m/z): M^+ calculated at 670.17, found at 670.39; Anal. Calcd for $C_{36}H_{32}F_2N_4OS_3$: C 64.45, H 4.81, N 8.35, S 14.34%; found: C 64.90, H 4.56, N 8.46, S 14.57%.

Synthesis of TRIr: bis[5-(6-(2,4-difluorophenyl)pyridine-3-yl)-4-octylthiophene-2-carbaldehyde]iridium(pentane-2,4-dione) dfppyTAIr (150 mg, 134 μmol) and 2-(3-ethyl-4-oxothiazolidin-2-ylidene)malononitrile (65 mg, 336 μmol) were stirred in the solvent with a mixture of anhydrous chloroform (10 mL) and triethylamine (0.1 mL) at room temperature for 12 h under a nitrogen atmosphere. Then the precipitate was extracted with CH_2Cl_2, washed with brine, dried over anhydrous $MgSO_4$, and concentrated under reduced pressure. The crude product was purified by chromatography on silica gel (eluent: dichloromethane) and wash with MeOH to yield the title compound as dark-red solid TRIr (139 mg, 70.5%). ^{1}H NMR (300 MHz, $CDCl_3$), δ (TMS, ppm): 8.62 (s, 2H), 8.31 (d, *J* = 9.0 Hz, 2H), 8.03 (s, 2H), 7.90 (d, *J* = 8.5 Hz, 2H), 7.37 (s, 2H), 6.36 (t, *J* = 10.1 Hz, 2H), 5.73 (d, *J* = 8.4 Hz, 2H), 5.45 (s, 1H), 4.31 (dd, *J* = 13.5, 6.6 Hz, 4H), 2.73 (t, *J* = 7.4 Hz, 4H), 1.86 (s, 6H), 1.62 (td, *J* = 14.2, 7.4 Hz, 4H), 1.40 (t, *J* = 7.0 Hz, 6H), 1.23-1.21 (m, 20H), 0.83 (t, *J* = 6.2 Hz, 6H). MALDI-TOF (m/z): M^+ calculated at 1466.36, found at 1465.02; Anal. Calcd for $C_{69}H_{65}F_4IrN_8O_4S_4$: C 56.50, H 4.47, N 7.64, S 8.74%; found: C 56.81, H 4.28, N 7.66, S 8.74%.

Synthesis of 2TRIr: bis[5′-(6-(2,4-difluorophenyl)pyridine-3-yl)-3-octyl-[2,2′-bithiophene]-5-carbaldehyde]iridium(2,2,6,6-tetramethylheptane-3,5-dione) dfppy2TAIr-tBu (200 mg, 147 μmol) and 2-(3-ethyl-4-oxothiazolidin-2-ylidene)malononitrile (71 mg, 367 μmol) were stirred in the solvent with a mixture of anhydrous chloroform (10 mL) and triethylamine (0.1 mL) at room temperature for 12 h under a nitrogen atmosphere. Then the precipitate was extracted with CH_2Cl_2, washed with brine, dried over anhydrous $MgSO_4$, and concentrated under reduced pressure. The crude product was purified by chromatography on silica gel (eluent: dichloromethane) and wash with MeOH to yield the title compound as reddish-brown solid 2TRIr (173 mg, 68.8%). ^{1}H NMR (300 MHz, $CDCl_3$), δ (TMS, ppm): 8.60 (s, 2H), 8.24 (d, *J* = 8.8 Hz, 2H), 7.97 (d, *J* = 11.4 Hz, 4H), 7.32 (d, *J* = 10.7 Hz, 6H), 6.40 – 6.32 (m, 2H), 5.87 (d, *J* = 8.5 Hz, 2H), 5.66 (s, 1H), 4.30 (dd, *J* = 13.2, 6.2 Hz, 4H), 2.88 – 2.79 (m, 4H), 1.68 (s, 4H), 1.40 (d, *J* = 6.6 Hz, 6H), 1.24 (s, 20H), 0.96 (s, 18H), 0.85 (s, 6H). MALDI-TOF (m/z): M^+ calculated at 1714.43, found at 1715.00; Anal. Calcd for $C_{83}H_{81}F_4IrN_8O_4S_6$: C 58.12, H 4.76, N 6.53, S 11.22%; found: C 58.17, H 4.69, N 6.53, S 10.77%.

NMR

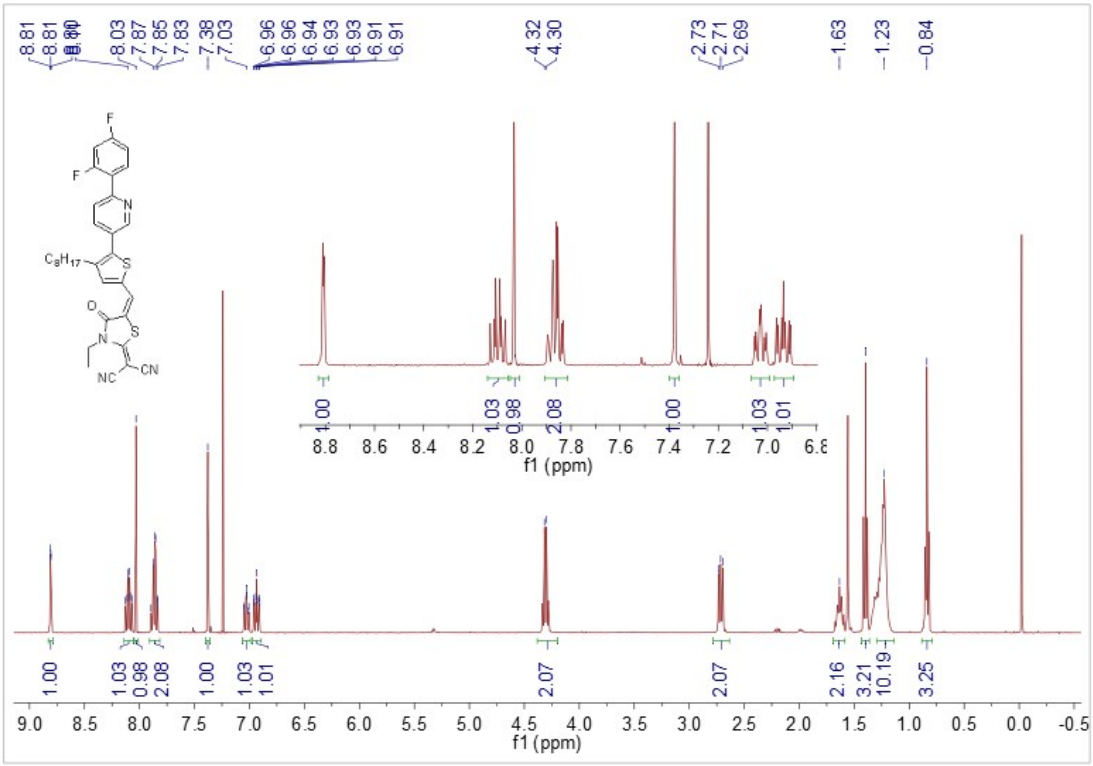

Fig. S1 (a) ^{1}H NMR Spectra: TR.

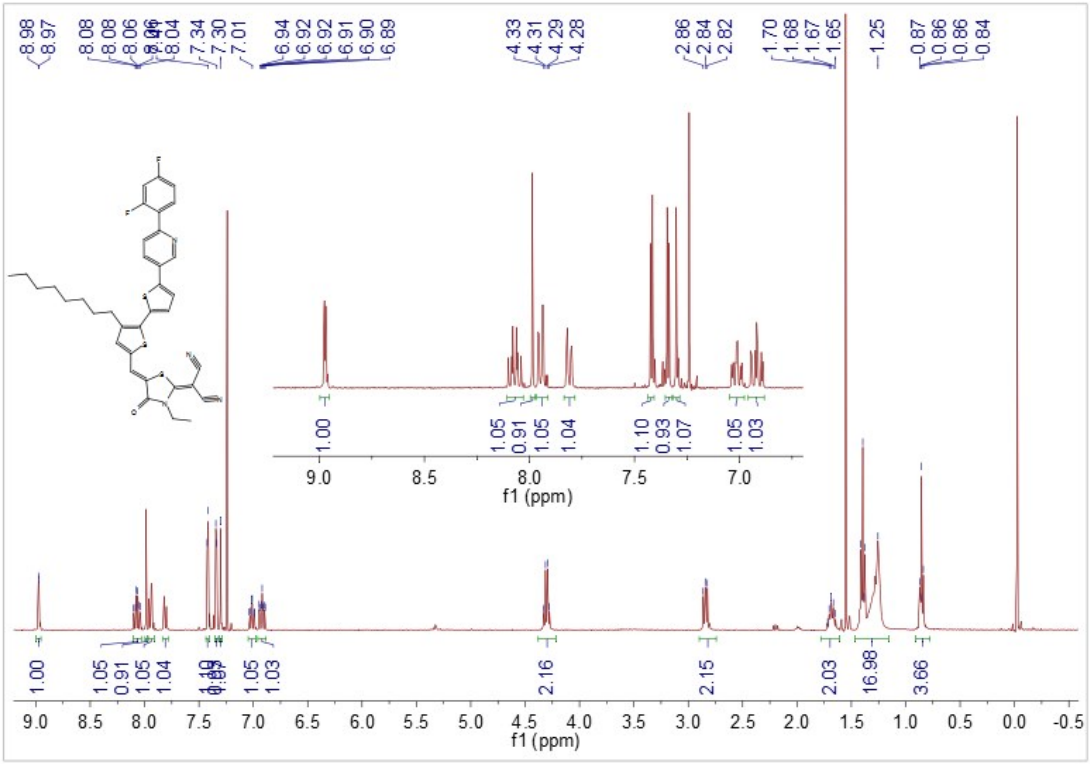

Fig. S1 (b) ^{1}H NMR Spectra: 2TR.

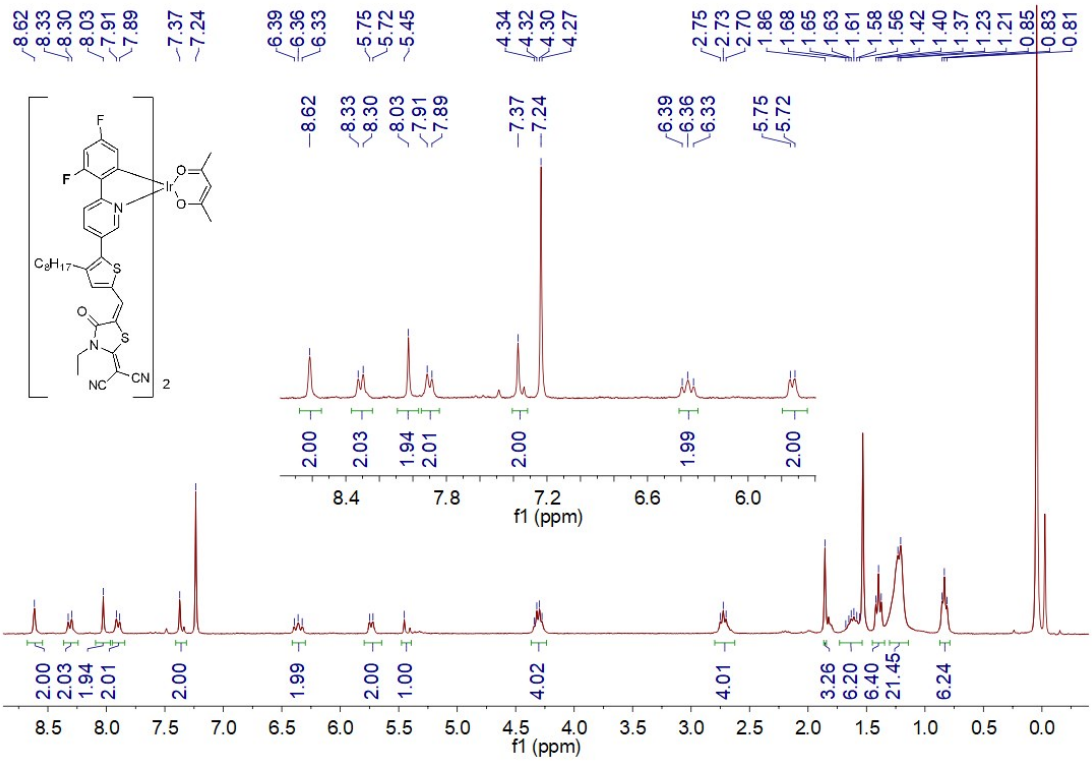

Fig. S1 (c) ^{1}H NMR Spectra: TRIr.

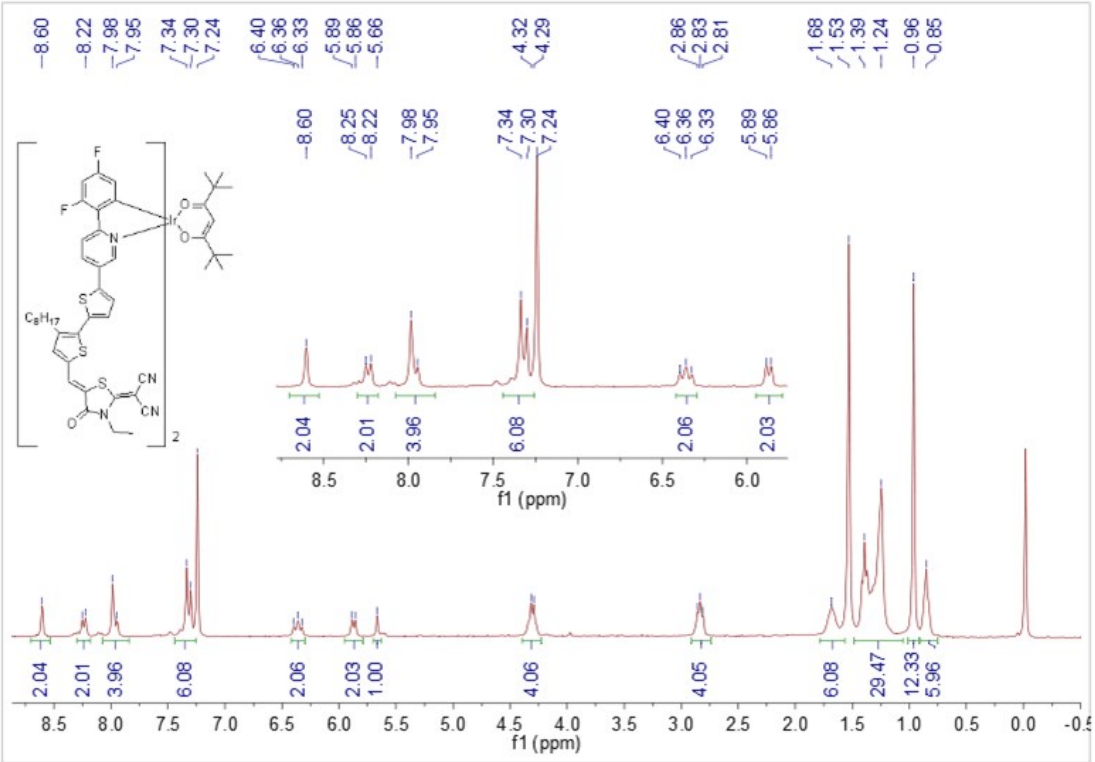

Fig. S1 d) ^{1}H NMR Spectra: 2TRIr.

Mass spectrometry

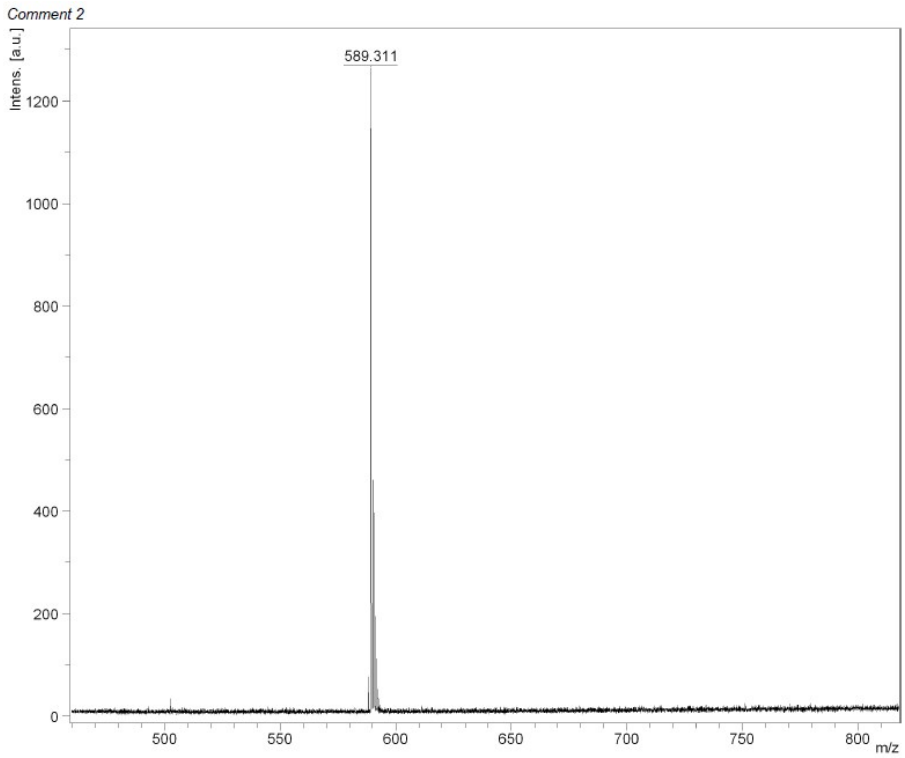

Fig. S2 (a) The mass spectrometry of TR.

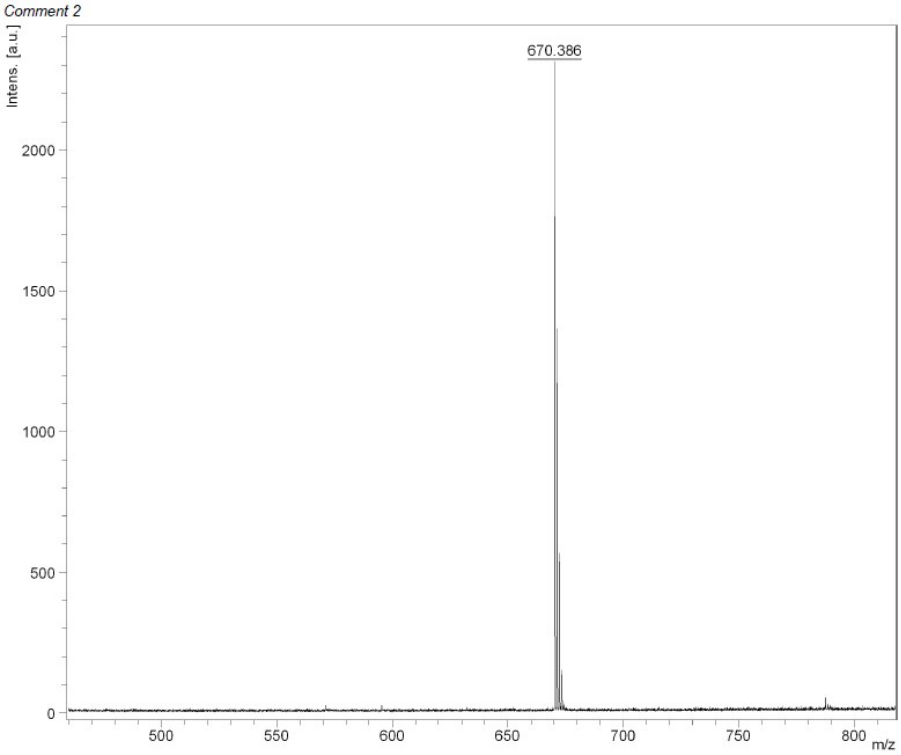

Fig. S2 (b) The mass spectrometry of 2TR.

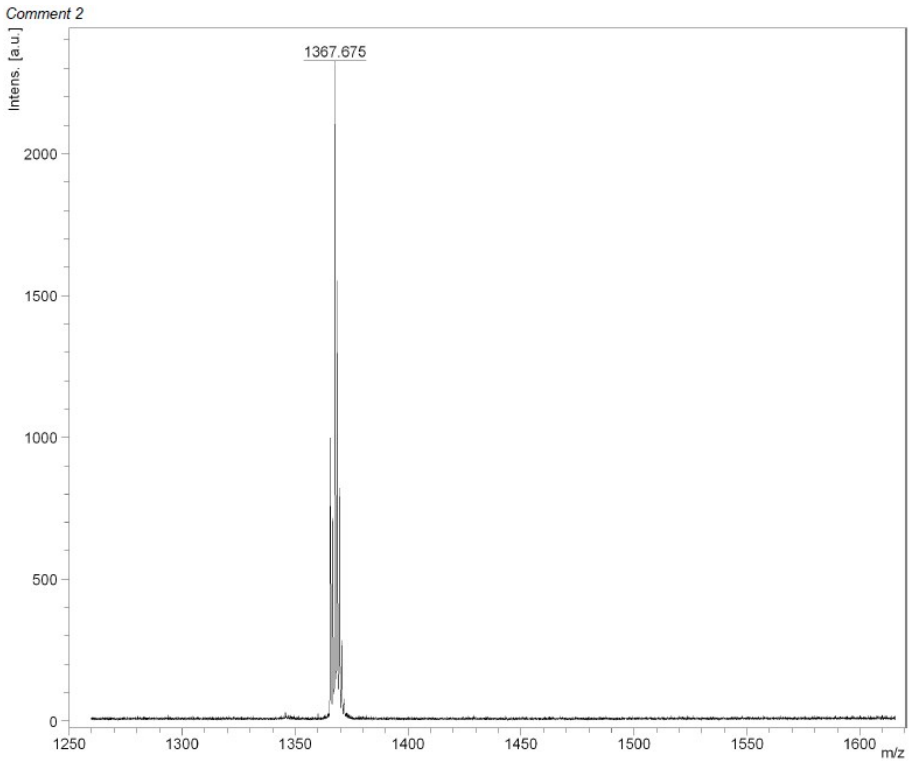

Fig. S2 (c) The mass spectrometry of TRIr.

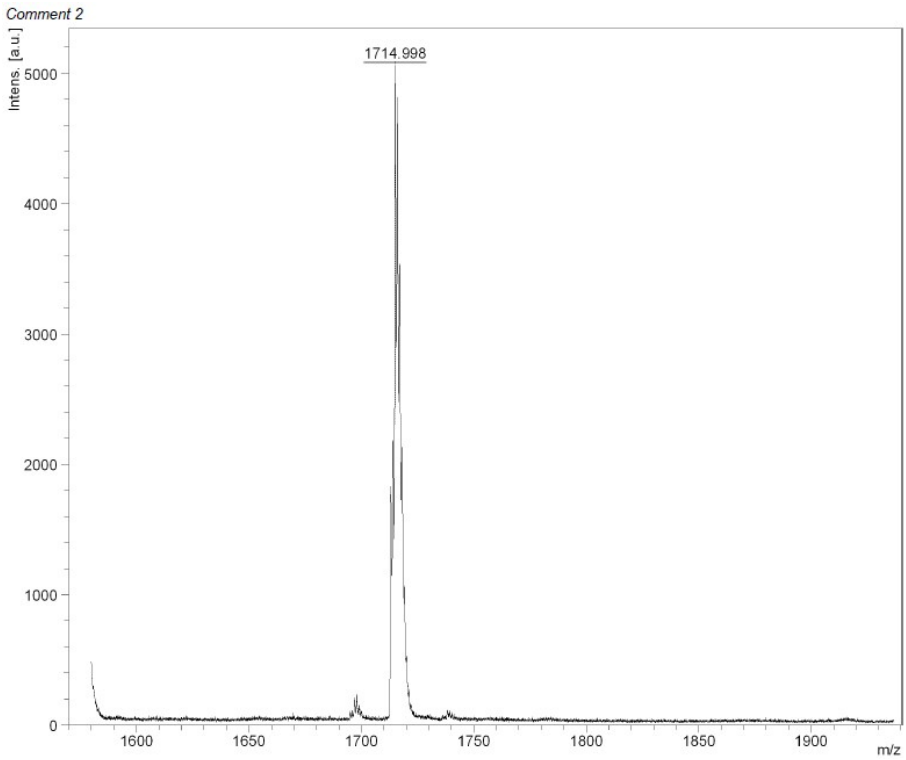

Fig. S2 (d) The mass spectrometry of 2TRIr.

Calculated molecular orbitals

Table S1 Frontier energy level distributions from DFT calculations.

Compounds	HOMO	LUMO
TR	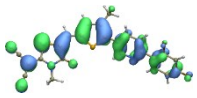	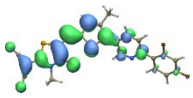
2TR	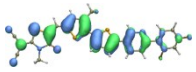	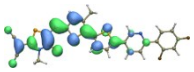
TRIr	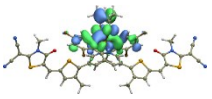	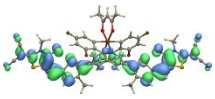
2TRIr	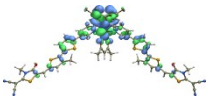	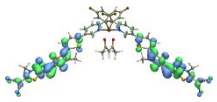

Thermal properties

The thermal stability of the samples was determined by measuring their weight loss at a heating rate of 10°C min^{-1} from 25 to 500°C using 3 mg sample under a nitrogen atmosphere.

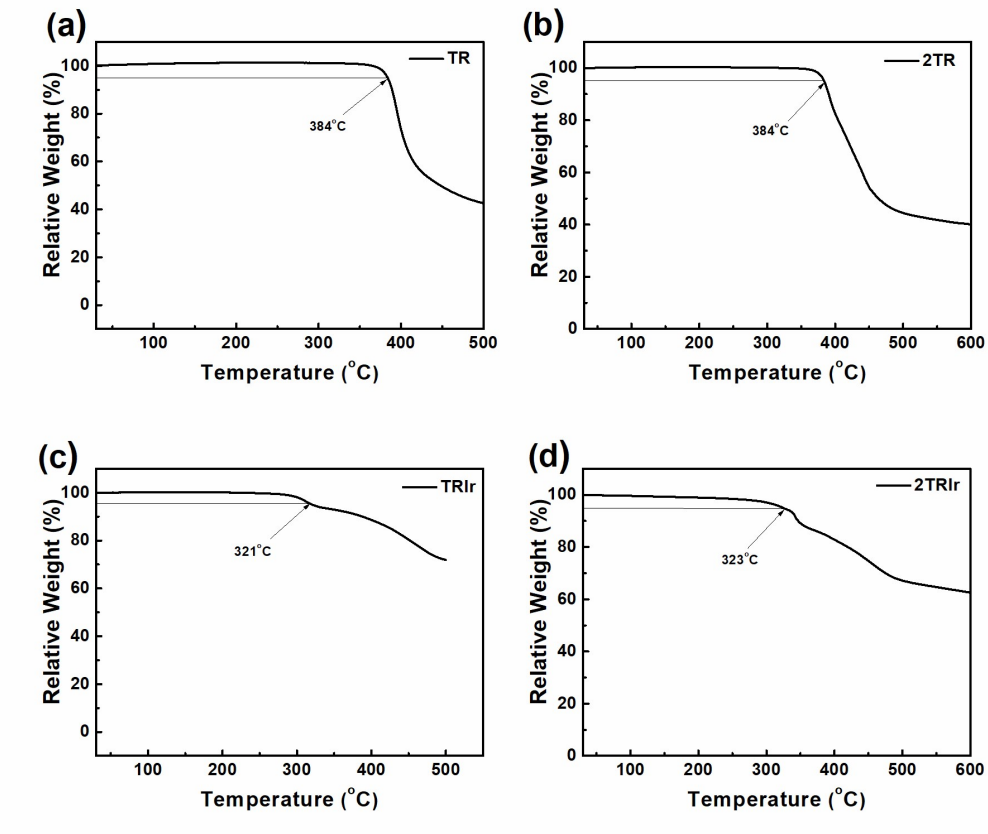

Fig. S3 TGA curves for compound (a) TR, (b) 2TR, (c) TRIr and (d) 2TRIr.

Electrochemical properties

The energy level of LUMO/HOMO for the four acceptors was measured by cyclic voltammetry (CV) using ferrocene as internal standard.

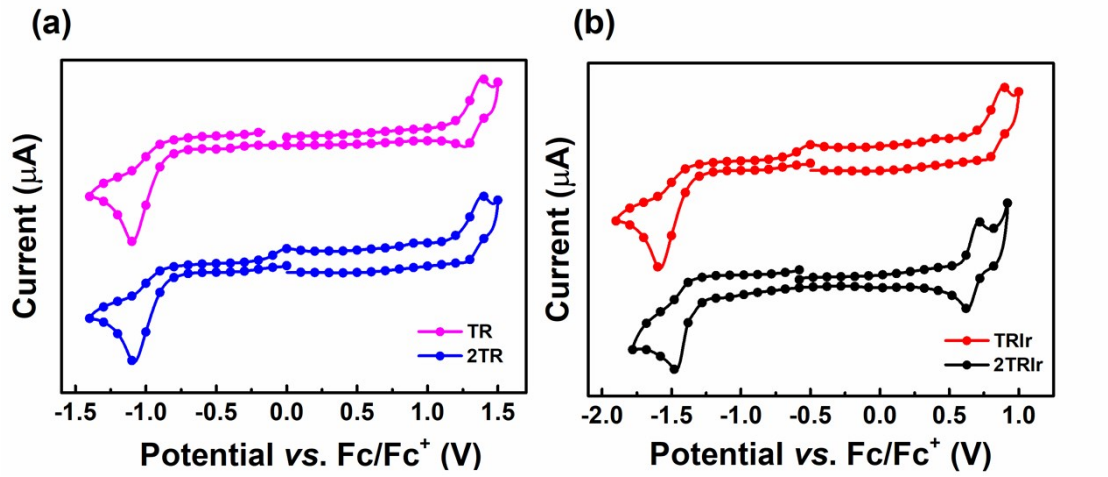

Fig. S4 Cyclic voltammograms of (a) TR and 2TR and (b) TRIr and 2TRIr in CH_3CN.

Time-resolved transient photoluminescence

The corresponding films were prepared by doping 30 wt% of acceptors into host matrix *m*-TPA-*o*-OXD.

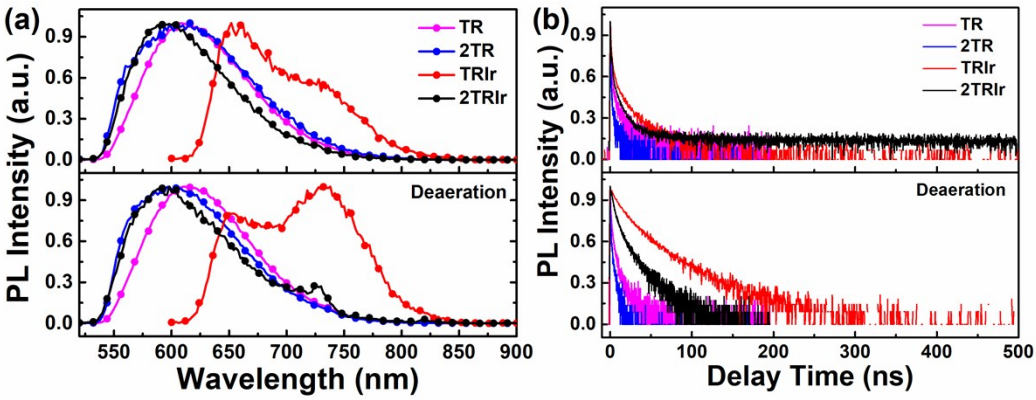

Fig. S5 PL spectra (a) and decay curves (b) in doped films by doping 30 wt% ratio of the corresponding compounds in *m*-TPA-*o*-OXD host matrix at ambient and deaeration conditions.

Table S2 Key PL data for the doped films.

Acceptors	λ_{PL}[a] [nm]	τ_1[a] [ns]/[%]	τ_2[a] [ns]/[%]	λ_{PL}[b] [nm]	τ_1[b] [ns]/[%]	τ_2[b] [ns]/[%]
TR	610	0.4/52.9	4.5/47.1	613	0.6/46.8	3.9/53.2
2TR	606	0.2/73.8	1.5/26.2	600	0.2/53.1	1.9/46.9
TRIr	655	0.4/73.6	5.4/26.4	653,730	10.7/50.3	34.8/49.7
2TRIr	595	0.3/62.8	2.8/37.2	595,727	4.0/62.0	15.7/38.0

[a] Measured in air condition. [b] Measured in degassed films.

OSC devices fabrication and measurement

OSCs with inverted structure of ITO/ZnO/active layer/MoO_3/Ag was fabricated as follows. Indium tin oxide (ITO) glass substrates were cleaned in an ultrasonic bath with detergent, deionized water, acetone and isopropanol, respectively, and followed by treatment of UV-ozone for 30 minutes. Then, ZnO was spin-coated on the ITO at 3500 rpm for 60 seconds and baked at 200°C for 60 min in air to give a film thickness around 30 nm. After that, the substrates with ZnO thin film were transferred to a nitrogen glove box. A mixture of PBDB-T:Ir complex was dissolved in CB/CN (100:1, v/v) mixed solvent (15 mg/mL) with stirring over 12 hours under 60°C. The ratios of content between donor and acceptor (D:A) were 0.8:1 and 1:0.8 for solution based on TRIr and 2TRIr, respectively. For ligand-based OSCs, blend of PBDB-T:TR or 2TR was dissolved in CB solvent (15 mg mL^{-1}, D:A=1:1) with stirring over 12 hours under 60°C. Then, the completely dissolved blend solution was spin-coated onto the ZnO layer to form bulk-heterojunction structure. A hole transport layer MoO_3 (10 nm) and an anode Ag (100 nm) was finally evaporated onto the surface of the active layer under vacuum (≈10^{-5} Pa) in sequence.

Table S3 Photovoltaic performance of the OSC devices based on PBDB-T:TRIr (D:A=0.8:1) with different thickness.

Thickness [nm]	V_{oc} [V]	J_{sc} [mA cm^{-2}]	FF	PCE [%]
47.9	0.89	3.47	0.37	1.08 (1.07±0.01)
71.1	0.89	3.58	0.37	1.20 (1.07±0.13)
85.4	0.89	2.34	0.36	0.77 (0.71±0.06)
94.1	0.86	2.34	0.35	0.71 (0.66±0.05)
125.9	0.86	1.19	0.38	0.40 (0.38±0.02)

Table S4 Photovoltaic performance of the OSC devices based on PBDB-T:2TRIr (D:A=1:0.8) with different thickness.

Thickness [nm]	V_{oc} [V]	J_{sc} [mA cm^{-2}]	FF	PCE [%]
60.5	0.92	4.83	0.35	1.52 (1.47±0.05)
63.6	0.92	5.02	0.35	1.62 (1.53±0.09)
75.4	0.92	4.12	0.34	1.29 (1.21±0.08)
93.0	0.89	3.86	0.33	1.13 (1.01±0.12)
124.9	0.89	2.47	0.33	0.73 (0.69±0.04)

Hole/electron-only devices fabrication and hole/electron mobility measurement

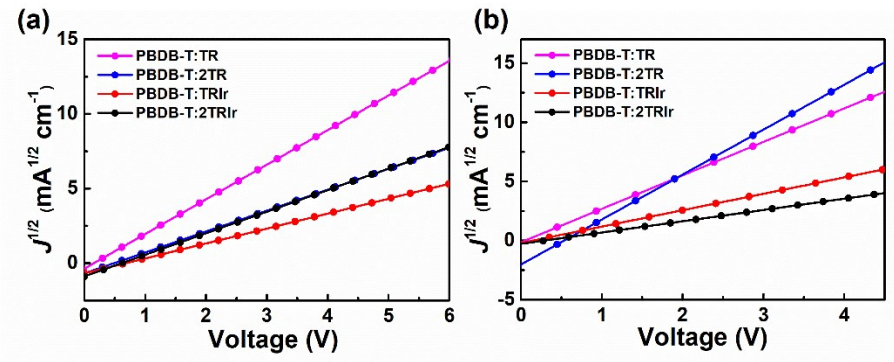

Fig. S6 $J^{1/2}$-V plots of (a) hole-only and (b)electron-only devices.